Journal of the Serbian Chemical Society
JSCS-info@shd.org.rs • www.shd.org.rs/JSCS
J. Serb. Chem. Soc. *87* (12) 1367–1380 (2022)
JSCS–5600
Original scientific paper
Published 18 November 2022

Transformation of fluorite δ-Bi_2O_3 into a new tetragonal phase

VLADIMIR V. ZYRYANOV* and SERGEY A. PETROV

Institute of Solid State Chemistry and Mechanochemistry, Siberian Branch of Russian Academy of Sciences, Novosibirsk, Kutateladze 18, 630090 Russian Federation

(Received 22 June, revised 12 August, accepted 21 September 2022)

Abstract: Bismuth oxide kinetically stabilized by doping with a metastable structure of disordered fluorite δ-Bi_2O_3 has a unique conductivity. Oxygen selective membranes at intermediate temperatures ~550 °C, on the base of cermet δ-Bi_2O_3/Ag, have the highest potential for air separation and can be used to produce oxygen for distributed multigeneration by burning fossil carbon fuels. When searching for the optimal composition of δ-Bi_2O_3, the degradation of fluorite into a new tetragonal phase was discovered in ceramics synthesized using mechanical activation. The tetragonal phase is formed and exists in a topotaxial composite with the fluorite structure. For a relatively stable over a wide temperature range tetragonal phase with a = 0.3854, c = 0.88905 nm, S.G. *P*-4, crystal structure and atomic coordinates have been proposed. In samples of fluorite and topotaxial composite, the Raman and Mössbauer spectra were recorded and discussed. The discovery of a new tetragonal phase of doped bismuth oxide and its existence area makes it possible to optimize the composition and the synthesis of a more stable solid electrolyte δ-Bi_2O_3 with high conductivity.

Keywords: Bi_2O_3 polymorphs; mechanical activation; solid state synthesis; powder XRD; Mössbauer spectroscopy; Raman spectroscopy.

INTRODUCTION

Bismuth oxide and Bi_2O_3-rich solid solutions exist in the form of several polymorphic modifications. All of them find applications in medicine, catalysis, materials science, *etc.*[1–5] However, great interest in this compound is associated primarily with the superionic properties of the high-temperature phase with the structure of disordered fluorite δ-Bi_2O_3.[1–4] Practical use of the unique oxygen conductivity of pure bismuth oxide is impossible due to its high reactivity and stability at t > 730 °C. Doping with cations of a smaller ionic radius makes it possible to kinetically stabilize the fluorite structure at lower temperatures with a

* Corresponding author. E-mail: vladinetta@academ.org
https://doi.org/10.2298/JSC220622075Z

partial deterioration of conductivity. The search for a composition and synthesis method of δ-Bi_2O_3 with optimal properties has been going on for a long time, but the results achieved so far do not provide practical implementation. Along with the experimental search, the theoretical studies are also carried out by first-principles calculations based on the density-functional theory DFT.[5] The generally accepted Bi_2O_3 polymorphs are listed in literature[6] and they are α-Bi_2O_3 with a monoclinic structure (stable at room temperature, S.G. $P2_1/c$, No. 14) and δ-Bi_2O_3 with a cubic structure (stable above 730 °C up to a melting point of 817 °C, S.G. *Fm*-3*m*, No. 225). When δ-Bi_2O_3 is cooled below 647 °C, a metastable β modification of the tetragonal structure is formed (S.G. $P\text{-}42_1c$, No. 114) and below 635 °C in an oxygen atmosphere γ modification of the cubic structure (sillenite, S.G. *I*23, No. 197) is formed. In addition to them, ε-Bi_2O_3 is also known, which is obtained by hydrothermal synthesis (S.G. *Pcnn*, No. 56, irreversibly transforms into the α-form at 400 °C), and ω-Bi_2O_3, which is formed on the BeO substrate. Theoretical studies were carried out on the basis of disordered fluorite with the ordering of oxygen vacancies along the <100>, <110>, and <111> directions, and combined superlattices.[6] The found polymorphic modifications with respect to the minimum energy relative to α-Bi_2O_3 were tested for stability. The approach used is supported by the fact that founded structure is very close to the experimentally observed phase ε-Bi_2O_3, called by the authors ε'-Bi_2O_3 (S.G. *Pbcn*, No. 60).[6] The existence of modifications with lining up of vacancies in the unit cell of fluorite is predicted to be tetragonal structures (S.G. $P4_2/mcm$, No. 132, and *P*-4*m*2, No. 115) and a cubic structure (S.G. *Pn*-3*m*, No. 224). In the model of vacancy superstructure 2×2×2, theoretically possible modifications were found: bixbyite observed for Y_2O_3, In_2O_3, Mn_2O_3 (S.G. *Ia*-3, No. 206), cubic (S.G. *Fd*-3*m*, No. 227) and trigonal (S.G. *R*3*m*, No. 160).

Optimization of the composition of δ-Bi_2O_3 fluorite is very important for practical applications because these materials exhibit the highest oxygen–ion conductivity of any material known to date. Doped with rare earth cations, δ-Bi_2O_3 retains disordered fluorite structure upon cooling down to room temperature. However, all known materials at about 600 °C undergo phase transformations with deterioration of their conductive properties.[7–11] The process of degradation of the fluorite structure (S.G. *Fm*-3*m*) begins with the ordering of oxygen vacancies along the <111> axis.[10] This change leads to an elongation of the lattice along the <111> axis and the transformation of fluorite into a rhombohedral phase (S.G. *R*-3) with the appearance of mechanical stresses that promote the segregation of dopants with the gradual formation of a rhombohedral phase (S.G. *R*-3*m*) or sillenite (S.G. *I*23).[11]

A relative failure of the theoretical method can be attributed to the discrepancy between the calculated and experimentally observed lattice parameters for known phases, which limits the reliability of the scientific forecasts. The prin-

ciple of searching for possible structures using the minimum energy is necessary but insufficient condition for the existence of phases, since under experimental conditions, the formation of a particular structure requires nucleation with subsequent growth. This stage is determined by kinetic factors. In this regard, it is *a priori* interesting to use mechanochemical synthesis or mechanical activation (MA), when the formation of products arranged in order at the contact of solid particles proceeds through the formation of mechanical loading above the threshold, so-called dynamic state, (D)*, in the form of growing rollers from an atomic mixture and then through its relaxation under quenching conditions.[12,13] As a result, the arranged products of certain structural types are formed, which have a high tolerance to changes in composition and a huge free volume of up to 9 % (vacancy defects).[11–13] The process of cumulative mass transfer, even at ambient temperature, is many orders of magnitude higher than the diffusion process at relatively high temperatures. This feature of the mechanochemical method makes it possible to detect crystal structures that were not observed due to kinetic limitations. Ultimately, the use of MA makes it possible to considerably accelerate the search for compositions of δ-Bi_2O_3 with an optimal combination of high oxygen conductivity and phase stability.

EXPERIMENTAL

For the synthesis of ceramic powders, the reagents from Russia and China were used in the form of oxides – Bi_2O_3 (purity >99.99 %) and Ta_2O_5 (>99.99 %), Dy_2O_3 and Er_2O_3 (>99.9 %), WO_3 (>99.9 %). Nitrates $Dy(NO_3)_3{\cdot}6H_2O$ and $Er(NO_3)_3{\cdot}6H_2O$ (>99.9 %), and $HfOCl_2$ (>99 %) were used as well. In the synthesis of some samples, a mixture of salts of highly charged cations (Hf, Ta, W, denoted as M^{5+} for brevity) was used to produce high-entropy ceramics. To introduce the Mössbauer isotope ^{57}Fe, Fe_2O_3 oxide was used with an isotope content of ~85 %, which was dissolved in a mixture of nitric and hydrochloric acid, followed by neutralization with ammonia to pH~3 and impregnation of MA powders, followed by drying.

The synthesis of ceramic powders was carried out in 3 cycles of grinding and firing at 800 to 950 °C. Dopants in the case of nitrates were introduced into MA bismuth oxide nanopowder by preliminary mixing in an agate mortar, followed by drying the resulting paste with gradual heating up to 600 °C until complete removal of water and nitrates. Mechanical processing of dry powders was carried out with steel balls of 4 mm in diameter in an AGO-2 planetary mill, Russia, with water-cooled steel jars (volume 2×150 ml) using a well-known technique.[8] Such method with pre-coating of the steel surface with ground ceramics and periodic mixing of material with balls provides a prominent reduction of iron contamination to <0.01 wt. % and an improvement in homogeneity. The treatment was carried out at the ratio of the mass of material and inox steel balls of 10–25 g/200 in an intensive mode of 60*g* (speed of rotation 750 rpm) in which the phenomenon of MA is accomplished. The supplied mechanical energy was 15–50 MJ/kg. Dense ceramics were obtained by pressing nanopowders at a pressure of 200 MPa and sintering at 950 °C for 1 min, cooling in furnace and air quenching from 820 °C to avoid cracking of a ceramic disk.

XRD studies (CuK_α radiation) were carried out on a diffractometer Bruker D8 Advance, Germany, using high-temperature (HT) camera HTK 1200N Anton Paar, Austria. Full-profile

Rietveld analysis of diffraction patterns was performed using the PowderCell 2.4 and Topas V4.2 software. The structure was visualized using Diamond-3 program. Mössbauer spectra were recorded at room temperature on an NZ-640 setup, Hungary, a γ-radiation source – ^{57}Co/Rh, a chemical shift relative to α-Fe. The spectra were processed using an original program developed in ISSCM SB RAS. Some powders and ceramics with fluorite and tetragonal phase were studied by Raman spectroscopy, using Bruker RFS100/s with NdYAl-laser, wavelength 1064 nm. To avoid possible errors, SEM studies of sintered ceramics and powders with EDS to control the composition were carried out on a TM-1000 microscope, Hitachi, Japan. Since the accuracy of weighing in the synthesis of compounds is much higher than the measurement error by the EDS method, the data on the estimated composition are not given. The EDS data obtained did not show the appearance of impurities and, within the experimental error, corresponded to the composition of the samples.

RESULTS AND DISCUSSION

XRD and structure

The diffraction patterns of $Bi_{0.76}Dy_{0.12}Er_{0.1}Hf_{0.02}O_{1.51}$ (DEH2) ceramics prepared from different precursors are shown in Figs. 1 and 2. The ceramics from oxide precursors are a composite of fluorite and a new tetragonal phase. According to the Rietveld full profile analysis, the crystallite sizes in ceramics fired at 850 °C are d = 116 for fluorite and 100 nm for tetragonal phase, with its fraction 35, 19, 18 and 27 % after heating to 400, 600, 700 and 950 °C, respectively. Fluorite lattice parameter was a_F = 0.54934(7) nm in single phase ceramics DEH2 with good homogenization of dopants and annealed free volume (Fig. 2), and in composite it was a_F = 0.5460(1) nm (Fig. 1, 950 °C), which means the segregation of dopants and the enrichment in tetragonal phase with Hf^{4+}.

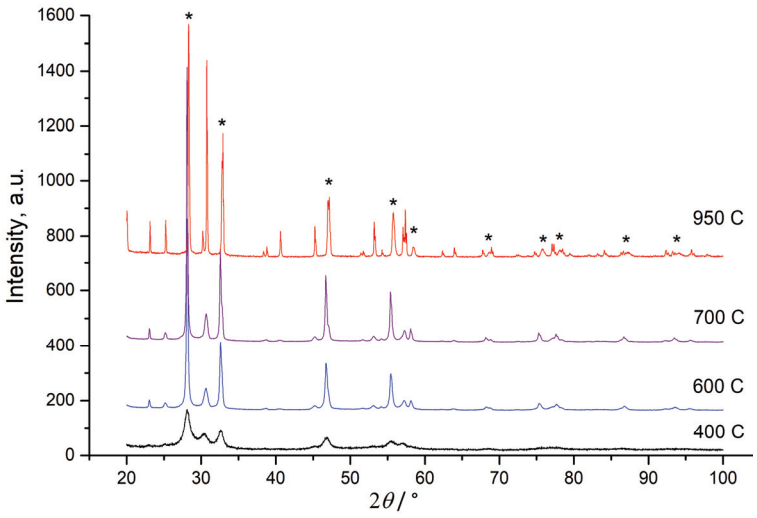

Fig. 1. Diffraction patterns of $Bi_{0.76}Dy_{0.12}Er_{0.1}Hf_{0.02}O_{1.51}$ ceramics after heating MA powders to different temperatures, asterisks indicate the peaks of fluorite.

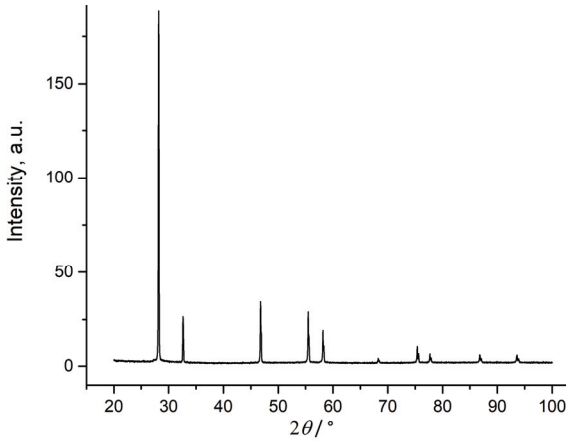

Fig. 2. Diffraction pattern of single-phase $Bi_{0.76}Dy_{0.12}Er_{0.1}Hf_{0.02}O_{1.51}$ fluorite, a = 0.54934(7) nm, synthesized from rare earth nitrates, sintered at 950 °C and air quenching.

The results of the Rietveld full profile analysis of DEH2 ceramics sample are shown in Fig. 3. All observed peaks of new phase are indicated in the tetragonal symmetry unit cell model (S.G. *P*-4, No. 81), Tables I and II, and the structure is shown in Fig. 4.

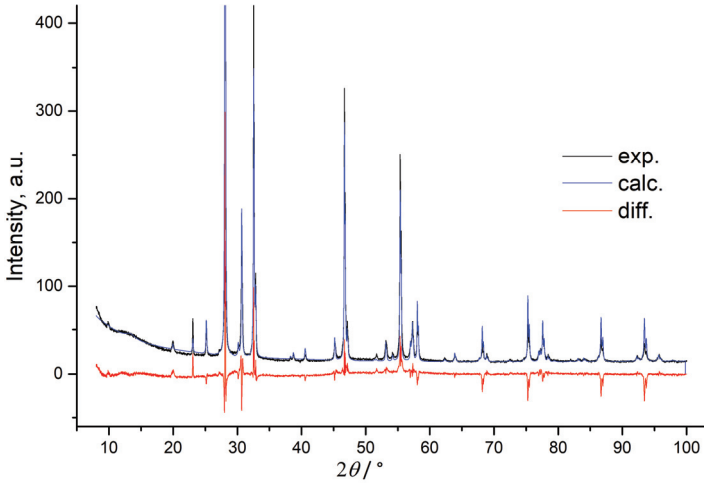

Fig. 3. Full-profile Rietveld analysis of diffraction pattern in topotaxial composite $Bi_{0.76}Dy_{0.12}Er_{0.1}Hf_{0.02}O_{1.51}$ after firing at 850 °C for 24 h. *R*-values for tetragonal phase: R_{wp} = 14.64, R_p = 10.91, *R*-Bragg = 7.568.

The structure of the tetragonal phase consists of fluorite-like layers separated by partially occupied polyhedron HfO_4 (FeO_4). The lattice parameters a_F = = 0.54982(1) nm, $\sqrt{2}a_t$ = 0.54341 nm, and the structures themselves are very

close. Therefore, there are grounds for asserting a topotaxial composite of fluorite and tetragonal phase. The formation of a tetragonal phase in contact with fluorite is similar to the formation ω-Bi_2O_3 on the BeO substrate.[6]

TABLE I. Atomic coordinates and occupation for the tetragonal phase in ceramics $Bi_{0.76}Dy_{0.12}Er_{0.1}Hf_{0.02}O_{1.51}$ after firing at 850 °C for 24 h (27 % of tetra phase, main phase fluorite with a = 0.54983 nm); space group, P-4, No 81; lattice parameters, a = 0.385405(24), c = 0.889047(98) nm; number of formula units, Z = 3.2; density, 8.7899(15)

Atom	Site	x	y	z	Occupation
Bi	2f	½	½	0.719	1
Bi(Dy,Er)	1a	0	0	0	0.799
Hf	1b	0	0	½	0.20
O1	2g	0	½	0.132	0.75
O2	2g	0	½	0.835	0.75
O3	2g	0	½	0.43	0.95

TABLE II. Interatomic distances

Atom 1	Atom 2	Distance, nm
Bi	O1	0.234
Bi	O2	0.219
Bi	O3	0.234
Bi(Dy,Er)	O1	0.226
Bi(Dy,Er)	O2	0.242
Hf	O3	0.203
O1	O2	0.274
O1	O3	0.265

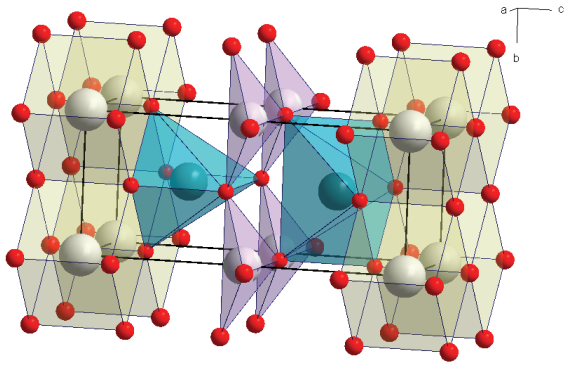

Fig. 4. Structure of tetragonal phase. Small dark balls – oxygen, big light balls – Bi, medium light balls – Hf, medium dark balls – Bi(Dy,Er).

The structure of the tetragonal phase suggests many variants of possible superlattices due to the low occupation of the position 1b by hafnium or other small cations, including iron. This circumstance is one of the possible reasons for the discrepancies in the observed and calculated peak intensities. This is con-

firmed by the presence of a halo in XRD patterns in the range of angles of 10 to 20°. In addition, the texturing of the samples adds discrepancy.

Existence area of the tetragonal phase

The combination of peaks at 19.9, 23.1, 25.2 and 30.7° is a good marker for the new tetragonal phase, which was observed as an impurity in many samples of stabilized δ-Bi_2O_3 obtained by high energy ball milling (MA) and doping with highly charged cations or small cations like Fe^{3+}, especially after prolonged annealing as a result of phase degradation of fluorite, Figs. 5 and 6. It can be assumed that the admixture of the tetragonal phase, due to the low intensity of the peaks, was incorrectly attributed to known phases in many works.

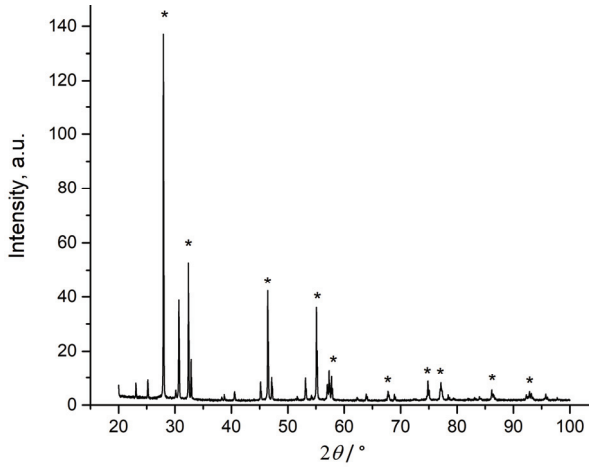

Fig. 5. XRD pattern of ceramics $Bi_{0.76}Dy_{0.12}Er_{0.09}(M^{5+})_{0.02}Fe_{0.01}O_{1.52}$ after heating to 950 °C and air quenching, asterisks indicate the peaks of fluorite. Topotaxial composite of fluorite 76 % and tetragonal phase 24 %; a_F = 0.55256(3) nm, d = 338(5) nm; a_t = 0.3854 ($\sqrt{2}a_t$ = 0.5449 nm), c = 0.88895(6) nm, d = 306(10) nm.

Diffraction patterns of powders and ceramics with different compositions and prehistories make it possible to reveal the existence area of tetragonal phase. Doping with highly charged cations Hf^{4+} at a level of 1 % gives a little effect on conductivity.[15]

When doping 3 % or more, non-conductive clusters are inevitably formed. Therefore, the minor doping in the development of a solid electrolyte was limited to 2 %. With the introduction of 2 % Ta^{5+} and W^{6+}, the tetragonal phase is not formed or is observed in trace amounts, due to the inhomogeneity of the samples, Fig. 6. This indicates the importance of the oxygen content for the formation of the tetragonal phase. At an oxygen content of ~1.50, the annealing of fluorite δ-Bi_2O_3 at t < 730 °C leads to the formation of sillenite, β-Bi_2O_3 or a rhombohedral phase. At an oxygen content >1.52, the structure of fluorite with a usual

coordination number of 8 for cations is stabilized much more efficiently. Therefore, the reasons for the degradation of metastable fluorite can be free volume, inhomogeneity, small cations, cationic diffusion and segregation, the outer and inner surfaces of ceramics in the form of pores. The tetragonal phase in topotaxial composites with fluorite is observed mainly at an oxygen content of 1.51––1.52. The formation of tetragonal phase during MA indicates stability in a wide temperature range, Figs. 1 and 5–7.

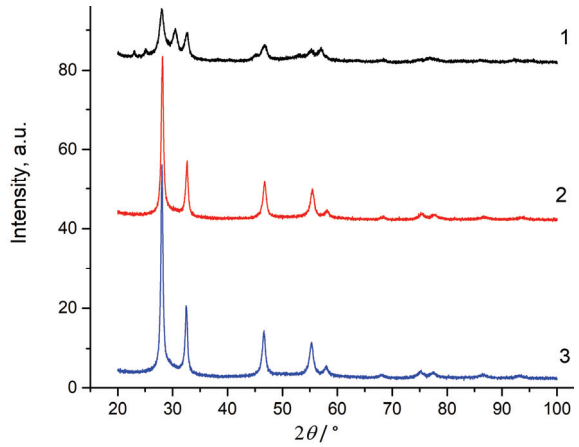

Fig. 6. Diffraction patterns of MA powders: 1 – topotaxial nanocomposite of fluorite and tetragonal phase $Bi_{0.765}Dy_{0.12}Er_{0.09}(M^{5+})_{0.02}Fe_{0.005}O_{1.52}$, 2 – fluorite $Bi_{0.76}Dy_{0.12}Er_{0.1}Ta_{0.02}O_{1.52}$, 3 – fluorite $Bi_{0.76}Dy_{0.12}Er_{0.1}W_{0.02}O_{1.53}$.

The diffraction patterns of Hf^{4+}-doped samples (EH2). after MA of powders and annealing at 400 °C are shown in Fig. 7. All powders are topotaxial composites of fluorite and tetragonal phase. A similar phenomenon of equilibrium of two phases during MA, the so-called mechanochemical equilibrium, was found in the $PbO–2WO_3$ and $PbO–2MoO_3$ systems.[13] The essence of this phenomenon is related to the formation and relaxation of (*D*)*.

According to the structure of the tetragonal phase, an increase in the content of Hf^{4+} should lead to an increase in the probability of its formation. However, $Bi_{0.7}Er_{0.2}Hf_{0.1}O_{1.55}$ ceramics with ideal homogenization obtained from nitrate precursors and a long three-stage firing at 800 °C without MA turned out to be a mixture of two fluorites with different hafnium content, Fig. 8. Nevertheless, the traces of the tetragonal phase appear in the diffraction patterns after annealing at 600 °C, as a result of degradation of metastable fluorite structure.

$Bi_{0.79}Er_{0.2}Hf_{0.01}O_{1.505}$ and $Bi_{0.77}Er_{0.2}Hf_{0.03}O_{1.515}$ ceramics (like EH2, 3 in Fig. 7) are positioned in the literature as the best solid electrolytes, which possess the conductivity of $Bi_{0.8}Er_{0.2}O_{1.50}$ ceramics while maintaining the structure of disordered fluorite and conductive properties after 1000 h of annealing at 600 °C,

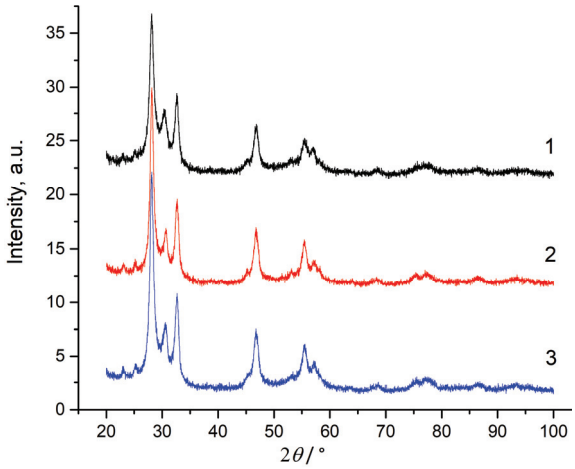

Fig. 7. Diffraction patterns of MA powders doped with Hf^{4+}, after annealing at 400 °C, topotaxial nanocomposites of fluorite and tetragonal phase: 1,2 – DEH2 from oxides and nitrates, respectively, 3 – EH2 from oxide.

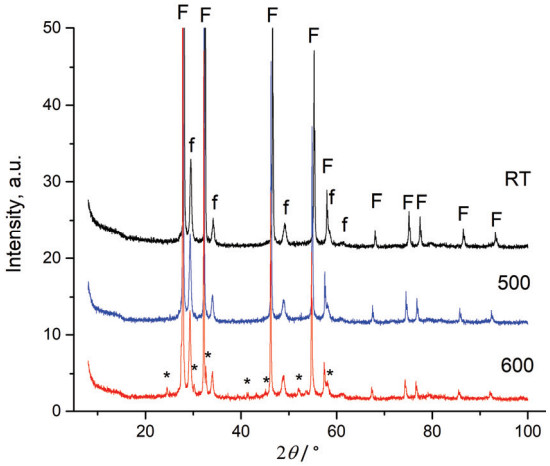

Fig. 8. HT XRD patterns of $Bi_{0.7}Er_{0.2}Hf_{0.1}O_{1.55}$ ceramics after sintering for 24 h at 850 °C at different temperatures, F and f – peaks of fluorites with a = 0.55072 and 0.52451 nm, asterisks indicate peaks of tetragonal phase.

due to hafnium doping.[15] For the fluorite structure degradation, only nuclei of the tetragonal phase are needed, which did not appear in dense homogenized ceramics, due to prolonged firing during synthesis and sintering (16 h at 890 °C).[16] When creating oxygen membranes based on δ-Bi_2O_3, such sintering conditions cannot be realized. Hafnium cations indeed stabilizes the fluorite structure due to slow diffusion.[14] However, the relatively small radius and charge of Hf^{4+} can lead to the appearance of nuclei of the tetragonal phase. The additional doping

with highly charged cations with a relatively large ionic radius can more effectively inhibit the formation of tetragonal phase nuclei.[11] The development of a solid electrolyte based on metastable fluorite ceramics by complex doping is within the framework of the concept of high-entropy ceramics (HEC).[11,14,16]

Mössbauer spectroscopy

The lowered doping of the ceramics with the ^{57}Fe isotope under the same conditions of synthesis yielded fluorite with a 3 % impurity of the tetragonal phase, which is insignificant for studies by γ-resonance spectroscopy, Fig. 9.

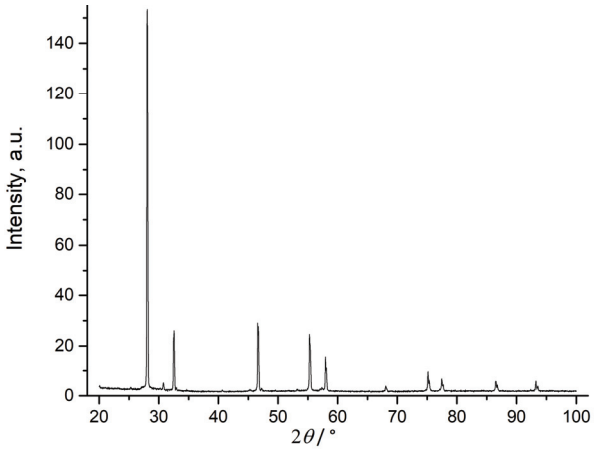

Fig. 9. Diffraction pattern of $Bi_{0.765}Dy_{0.12}Er_{0.09}(M^{5+})_{0.02}Fe_{0.005}O_{1.52}$ ceramics, synthesized from nitrates, sintered at 950 °C and air quenching. Fluorite, a = 0.55080(4) nm, tetragonal phase.

Mössbauer spectra of $Bi_{0.765}Dy_{0.12}Er_{0.09}(M^{5+})_{0.02}Fe_{0.005}O_{1.52}$ fluorite ceramics after heating to 950 °C and air quenching, and topotaxial composite of fluorite and tetragonal phase after synthesis and 8 min MA (Fig. 6, 1), are shown in Fig. 10, 1 and 2, respectively. The spectra are represented by doublets differing in parameters (Table III), which correlates with different structures. In a fluorite sample with a lattice parameter a_F = 0.55080(4) nm, a relatively small chemical shift, δ = 0.25 mm s^{-1} and quadrupole splitting, ε = 0.77 mm s^{-1} indicates low Fe^{3+} coordination or large distances to oxygen atoms, Fig. 10 (1). In a cerium dioxide nanopowder with a fluorite structure (a_F = 0.5401 nm) doped with 10 % molar Fe^{3+}, a similar doublet with δ = 0.24 mm s^{-1} and ε = 0.95 mm s^{-1} was observed.[17] It is most likely that Fe^{3+} has an octahedral environment. In fluorite $CeZrO_4$ (a_F = 0.526 nm) with the occupied oxygen positions, the spectrum parameters δ = 0.33 mm s^{-1} and ε = 1.09 mm s^{-1} are significantly different.[18] The authors believe that iron ions locally deform the lattice.[17] Taking

into account all the results, it is most likely that small Fe^{3+} ions in the fluorite lattice occupy cation positions with the distortion of the local environment.

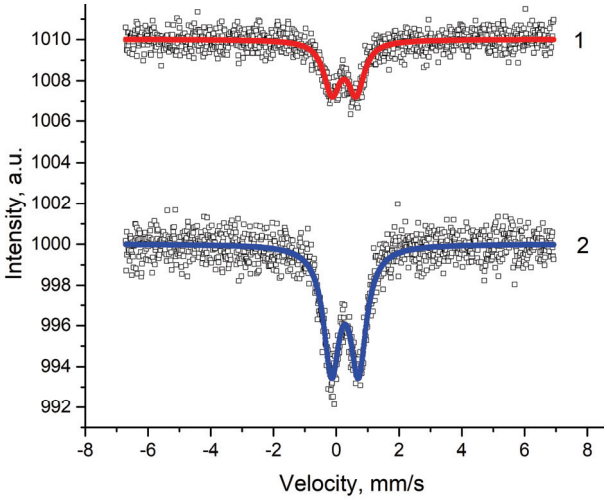

Fig. 10. Mössbauer spectra of ^{57}Fe in $Bi_{0.765}Dy_{0.12}Er_{0.09}(M^{5+})_{0.02}Fe_{0.005}O_{1.52}$ sample after firing at 950 °C and air quenching with fluorite structure (1) and after synthesis and 8 min MA, topotaxial nanocomposite of fluorite and tetragonal phase (2).

TABLE III. Parameters of $^{57}Fe^{3+}$ Mössbauer spectra at room temperature of samples with composition $Bi_{0.765}Dy_{0.12}Er_{0.09}(M^{5+})_{0.02}Fe_{0.005}O_{1.51}$

Structure	Conditions of preparation	Line width, mm s^{-1}	δ / mm s^{-1}	ε / mm s^{-1}
Fluorite	950 °C, air quenching	0.62(1)	0.25(1)	0.77(2)
Tetra-phase	950 °C , MA 8 min	0.61(1)	0.28(1)	0.86(2)

In the topotaxial composite of fluorite and tetragonal phase, like ω-Bi_2O_3 on the BeO substrate, the main part of the introduced iron is segregated in the tetragonal phase, as evidenced by its formation when even a small impurity of 0.5 % molar Fe^{3+} is introduced into a relatively stable fluorite. In the tetragonal phase, the chemical shift is slightly larger (δ = 0.28 mm s^{-1}) than in fluorite, Fig. 10 (2), but it is still noticeably smaller than the usual chemical shift for $Fe^{3+}O_6$. In the tetragonal phase, Fe^{3+} is uniquely located in the centre of the tetrahedron with a distance of ~0.203 nm to oxygen ions, Fig. 4. The parameters of doublet δ = 0.28 mm s^{-1} and ε = 0.86 mm s^{-1} are close to those of 5-coordinated Fe^{3+} in MA perovskites (δ = 0.29 and ε = 1.19).[14] For comparison, parameters of doublet of the $Fe^{3+}O_6$ states in perovskites were δ = 0.34 to 0.35 mm s^{-1}, ε = 0.57 to 0.66 mm s^{-1}, and a distance Fe-O 0.193 nm.[14] Parameters of doublet of $Fe^{3+}O_4$ in mullite-like structure $Bi_2Fe_4O_9$ were δ = 0.231 mm s^{-1} and ε = 0.95 mm s^{-1} (0.352 and ~0.95 mm s^{-1} for $Fe^{3+}O_6$).[19]

Raman spectroscopy

The Raman spectra of fluorite and topotaxial composite are shown in Fig. 11.

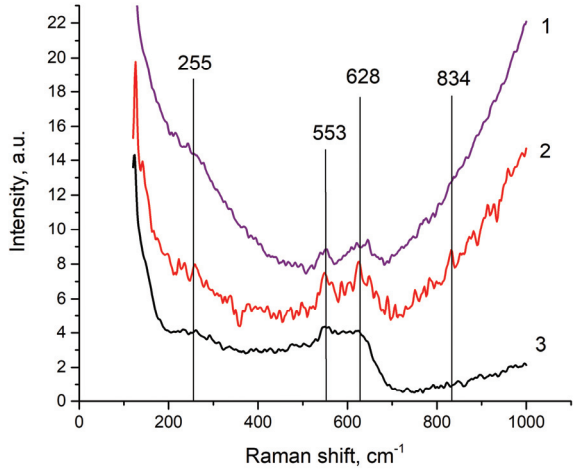

Fig. 11. Raman spectra with accumulation time 60, 10 and 10 min respectively: 1) MA powder DEH2 after heating up to 700 °C (topotaxial nanocomposite of fluorite with tetragonal phase, Fig. 1), 2) EH2 ceramics with fluorite structure, after synthesis at 900 and sintering at 700 °C, 3) the same EH2 sample after MA 8 min, nanopowder with fluorite structure.

Spectra exhibit broad bands at 255, 553, 628 and a very weak sharp band at 834 cm^{-1} at the noise level and only in EH2 ceramics. In fluorite δ-Bi_2O_3, stabilized with 20 mol. % Nb^{5+} or Ta^{5+}, two broad bands are observed at 550 and 320 cm^{-1},[20] which are attributed to Bi–O stretches with interatomic distances of 0.226 and 0.204 nm in 5-fold coordination, and a sharp band at 821 cm^{-1}. A similar band was found in sillenite and is attributed to the $Bi^{5+}O_4$ tetrahedron.[20] In stabilized EH2 fluorite, a greater number of bands is related to high content of oxygen vacancies relative to $Bi_{0.8}Ta_{0.2}O_{1.7}$, which leads to different states. On the whole, no new bands were found in the topotaxial composite of fluorite and the tetragonal phase, and the bands common to fluorite have a very weak intensity. The absence of bands that could be attributed to the tetragonal phase can be associated with a large number of possible states with low symmetry, in addition to being in the field of mechanical stress due to topotaxial bonding with fluorite.

CONCLUSION

A new tetragonal phase of doped bismuth oxide as a degradation product of the disordered fluorite structure δ-Bi_2O_3 was found in a topotaxial composite with fluorite. The tetragonal phase is stable over a wide temperature range. The free volume arising during MA and inhomogeneous doping promote the form-

ation of nuclei of the tetragonal phase. The area of existence of the tetragonal phase in doped bismuth oxide is determined by the oxygen content of approximately 1.51 to 1.52 and the content of minor dopants ~0.01 to 0.05 with a small ionic radius, including Hf^{4+} and Fe^{3+}. The structure of the tetragonal phase is proposed on the basis of powder XRD data, which can form superlattices when arranged. The Mössbauer and Raman spectra are in agreement with the proposed structure. The data obtained make it possible to optimize the composition of the solid electrolyte and the conditions for its synthesis for the kinetic stabilization of the fluorite structure. Possible contamination of the solid electrolyte with iron, hafnia (or zirconia) during MA and grinding, as well as other cations upon contact with certain components of oxygen membranes, promotes phase degradation of metastable fluorite δ-Bi_2O_3.

Acknowledgements. This work was supported by the Russian Foundation for Basic Research, Grant 20-03-00349, and within the framework of the state assignment of the Institute of Solid State Chemistry and Mechanochemistry, SB RAS (project 0301-2019-0002).

ИЗВОД

ТРАНСФОРМАЦИЈА ФЛУОРИТА δ-BI_2O_3 У НОВЕ ТЕТРАГОНАЛНЕ ФАЗЕ

VLADIMIR V. ZYRYANOV и SERGEY A. PETROV

Institute of Solid State Chemistry and Mechanochemistry, Siberian Branch of Russian Academy of Sciences, Novosibirsk, Kutateladze 18, 630090 Russian Federation

Бизмут(III)-оксид, кинтетички стабилизаван додатком неуређене метастабилне структуре флуорита, има изузетно велику проводљивост. Селективне кисеоничне мембране, применом кермет (cermet) Bi_2O_3/Ag композитног материјала на температури од око 550 °C, имају највећи потенцијал за сепарацију ваздуха и могу се употребити за мултифункционалну производњу кисеоника на бази сагоревања фосилних угљеничних горива. Приликом истраживања оптималног састава δ-Bi_2O_3, нађено је да у керамици која је синтетисана механичком активацијом долази до деградације флуорита у нове тетрагоналне фазе. Тетрагонална фаза постоји у топотаксијалном композиту структуре флуорита. За тетрагоналну фазу са a = 3,854 nm, c = 0,88905 nm и S.G. P-4, која је релативно стабилну у широком температурском опсегу, предложена је кристална структура и атомске координате. За узорке флуорита и топотаксијалне композите дискутовани су њихови Raman и Mössbauer спектри. Откриће нове тетрагоналне фазе допираног бизмут(III)-оксида и подручја његове оптималне стабилности омогућава оптимизацију састава и синтезу стабилнијег чврстог електролита δ-Bi_2O_3 са великом проводљивости.

(Примљено 22. јуна, ревидирано 12. августа, прихваћено 21. септембра 2022)

REFERENCES

1. H. A. Harwig, A.G. Gerards, *J. Solid State Chem*. **26** (1978) 265 (https://dx.doi.org/10.1016/0022-4596(78)90161-5)
2. P. Shuk, H. D. Wiemhofer, U. Guth, W. Gopel, M. Greenblatt, *Solid State Ionics* **89** (1996) 179 (https://dx.doi.org/10.1016/0167-2738(96)00348-7)

3. V. V. Kharton, F. M. B. Marques, A. Atkinson, *Solid State Ionics* **174** (2004) 135 (https://dx.doi.org/10.1016/j.ssi.2004.06.015)
4. B. Singh, S. Ghosh, S. Aich, B. Roy, *J. Power Sources* **339** (2017) 103 (https://dx.doi.org/10.1016/j.jpowsour.2016.11.019)
5. A. Dapčević, D. Poleti, L. Karanović, J. Miladinović, *J. Serb. Chem. Soc*. **82** (2017) 1433 (https://doi.org/10.2298/JSC170711111D)
6. A. Matsumoto, Y. Koyama, I. Tanaka, *Phys. Rev., B* **81** (2010) 094117 (https://dx.doi.org/10.1103/PhysRevB.81.094117)
7. N. Jiang, R. M. Buchanan, F. E. G. Henn, A. F. Marshall, D. A. Stevenson, E. D. Wachsman, *Mater. Res. Bull*. **29** (1994) 247 (https://doi.org/10.1016/0025-5408(94)90020-5)
8. S. Boyapati, E. D. Wachsman, N. Jiang, *Solid State Ionics* **140** (2001) 149 (https://doi.org/10.1016/S0167-2738(01)00698-1)
9. S. Boyapati, E. D. Wachsman, B. C. Chakoumakos, *Solid State Ionics* **138** (2001) 293 (https://doi.org/10.1016/s0167-2738(00)00792-x)
10. E. D. Wachsman, *J. Eur. Ceram. Soc*. **24** (2004) 1281 (http://dx.doi.org/10.1016/s0955-2219(03)00509-0)
11. V. V. Zyryanov, A. S. Ulihin, *Ceram. Int*. **48** (2022) 16877 (https://doi.org/10.1016/j.ceramint.2022.02.242)
12. V. V. Zyryanov, *Inorg. Mater*. **41** (2005) 378 (http://dx.doi.org/10.1007/s10789-005-0140-y)
13. V. V. Zyryanov, *Russ. Chem. Rev*. **77** (2008) 105 (https://doi.org/10.1070/RC2008v077n02ABEH003709)
14. V. V. Zyryanov, S. A. Petrov, A. S. Ulihin, *Ceram. Int*. **47** (2021) 29499 (https://doi.org/10.1016/j.ceramint.2021.07.118)
15. B.-H. Yun, C.-W. Lee, I. Jeong, K. T. Lee, *Chem. Mater*. **29** (2017) 10289 (https://doi.org/10.1021/acs.chemmater.7b03894)
16. A. J. Wright, J. Luo, *J. Mater. Sci*. **1000** (2020) 9812 (https://doi.org/10.1007/s10853-020-04583-w)
17. F. F. H. Aragon, J. C. R. Aquino, J. E. Ramos, J. A. H. Coaquira, I. Gonzalez, W. A. A. Macedo, S. W. da Silva, P. C. Morais, *J. Appl. Phys*. **122** (2017) 204302 (https://doi.org/10.1063/1.4999457)
18. R. Nedyalkova, D. Niznansky, A-C. Roger, *Catal. Comm*. **10** (2009) 1875 (http://dx.doi.org/10.1016/j.catcom.2009.06.017)
19. A. Kirsch, M. M. Murshed, F. J. Litterst, T. M. Gesing, *J. Phys. Chem., C* **123** (2019) 3161 (http://dx.doi.org/10.1021/acs.jpcc.8b09698)
20. F. D. Hardcastle, I. E. Wachs, *J. Solid State Chem*. **97** (199) 319 (https://doi.org/10.1016/0022-4596(92)90040-3).